Energy Losses of Muons, Pions, Protons, and Deuterons Channeled in Si

J. E. Valdés,[1] P. Vargas,[2] and N. R. Arista[3]

[1]*Departamento de Física, Universidad de Santiago de Chile, Avenida Ecuador 3493, Santiago, Chile*
[2]*Departamento de Física, Universidad Técnica Federico Santa María, Valparaíso, Chile*
[3]*Centro Atómico Bariloche, Instituto Balseiro, CNEA, Bariloche, Argentina*

(Received 13 January 2000)

The energy loss of positive muons, pions, protons, and deuterons channeled in Si crystals has been investigated by computer simulation. The model considers the individual trajectories of particles inside the target and calculates the electronic energy loss for each particle history. The results show important differences in the energy loss distributions, stopping powers, and straggling values for low and intermediate energies, as a consequence of channeling effects.

PACS numbers: 61.85.+p, 34.50.Bw, 34.50.Fa

The use of positive pions and muons as probes in condensed matter has been a subject of increasing interest during the last decade, giving rise to new spectroscopies and applications in material science [1–3], particularly in relation to hydrogen studies [4,5]. A useful technique developed for this purpose is based on channeling-blocking experiments [4,6].

Since the masses of these particles are much larger than the electron mass, the slowing down process is usually described assuming equal electronic stopping powers for the same velocity of the various particles. Therefore, the usual proton stopping models and empirical approximations [7] are applied to describe this process [3,4].

The phenomenon of channeling provides a special situation [8]. In particular, one may expect a direct influence of the particle mass in determining the dynamics of the trajectories, and therefore a corresponding effect on the energy-loss spectra of channeled particles. The purpose of this work is to make a comparative study of the energy loss distributions, stopping powers, and straggling, for channeled deuterons, protons, positive pions, and muons, and to show differences induced by lattice steering effects.

The basic models to describe the channeling and energy loss process have been explained before [9]. The model includes a band-structure calculation using the tight-binding linear muffin-tin method [10] to obtain the electron density within the channel and the electronic density of states [9]. The simulation of particle trajectories is made by solving Newton's equations of motion using the Runge-Kutta method. The electronic energy loss is included explicitly in the dynamics of the particle using the instantaneous energy calculated in a continuous slowing down process, and subject also to a spread of energy determined by the energy straggling effect.

In order to cover a wide range of energies, the calculation of the energy loss for channeled particles is based on two previous formulations: the linear-response or dielectric formalism, and the nonlinear, or transport cross section model, more adequate for low velocities.

The mean energy loss $S \equiv \langle dE/dx \rangle$ of a particle with charge Z_1 and velocity v is usually calculated in terms of the dielectric function $\varepsilon(q, \omega; r_s)$ as follows [11]:

$$S = \frac{2}{\pi} \frac{Z_1^2 e^2}{v^2} \int \frac{dq}{q} \int_0^{qv} \omega \, d\omega \, \mathrm{Im}\left[\frac{-1}{\varepsilon(q, \omega; r_s)} \right], \quad (1)$$

where r_s is the usual one-electron radius, related to the electron density n and Fermi velocity v_F by $r_s^3 = 3/4\pi n$, $v_F = 1.919/r_s$. Useful approximations for low and high velocities have been derived before [11]. It is known, however, that for low velocities nonlinear corrections become important [12], and so the dielectric model will be used here to describe only the range of intermediate ($v \sim v_F$) and high ($v \gg v_F$) velocities.

In the low-velocity range ($v \ll v_F$) we use a more accurate nonlinear approximation, where the stopping power is given by [12]

$$S_{\mathrm{low}} = nmvv_F \sigma_{\mathrm{tr}}(v_F), \quad (2)$$

where $\sigma_{\mathrm{tr}}(v_F)$ is the transport cross section, calculated quantum mechanically in terms of phase shifts $\delta_l(v_F)$, which are numerically determined by solving Schrödinger's equation for the scattering of electrons using a self-consistent model to adjust the screened potential [9].

By comparing the results from these two methods, we have found that a simple matching between the nonlinear results for low energies, and the intermediate and high-energy values from dielectric theory, may be obtained in the form $S(v, v_F) = S_{\mathrm{low}} S_{\mathrm{high}} / (S_{\mathrm{low}}^2 + S_{\mathrm{high}}^2)^{1/2}$. This provides a reasonably good approximation on a wide range of velocities and is appropriate for comparative purposes in the present simulations.

In a similar way we include the quantum fluctuations or energy loss straggling following this picture. Here the low-energy straggling, Ω_{low}, is given by [13]

$$\Omega_{\mathrm{low}}^2(k_F) = 3nv^2 v_F^2 \delta x \int d\sigma(v_F, \theta) \sin^3(\theta/2), \quad (3)$$

where δx is an infinitesimal displacement of the particle in each step of its motion along the trajectory, and $d\sigma$ is the differential scattering cross section calculated also from the phase shifts $\delta_l(v_F)$.

On the other hand, in the case of high energies we may use Bohr's approximation to the energy straggling,

$\Omega^2_{\text{high}}(k_F) = 4\pi Z_1^2 n \delta x$. Finally, the straggling at all energies may be calculated by a quadratic interpolation similar to the one used for the stopping, $\Omega = \Omega_{\text{low}}\Omega_{\text{high}}/(\Omega^2_{\text{low}} + \Omega^2_{\text{high}})^{1/2}$.

To account for the differences between channeling and random energy loss we also calculate the random average of the energy loss by integrating over the electron density profile using the local-density approximation [14],

$$\langle S \rangle = 4\pi N_a \int_0^{r_a} r^2 S(v, v_F[r])\, dr\,, \qquad (4)$$

where N_a is the atomic density and r_a is the atomic-cell radius of the solid.

We performed a series of calculations of particle trajectories in a wide range of incident energies ($0.1 \leq v/v_0 \leq 10$ a.u.). We used a uniform random distribution of initial impact parameters in the XY plane perpendicular to the channel axis Z. Each simulation included 10^5 histories. The energy loss distributions were obtained for all the particles emerging from the crystal within a small angular acceptance cone of 0.5°, and the corresponding mean energy losses were determined.

In Fig. 1 we show a sample of trajectories for protons and muons with incident velocities $v = 2$ a.u. channeled on a 814.2 Å-thick Si crystal; the trajectories are projected on the ZX plane, where Z is the $\langle 100 \rangle$ direction and $X = 0$ corresponds to the channel axis. The figure illustrates the different characteristics of channeling of particles with various masses. Channeling of lighter particles (pions and muons) shows oscillating trajectories with shorter periods as compared with same-velocity deuterons and protons. This behavior is in agreement with the predictions of Lindhard's channeling model [15] and with previous studies of ion channeling trajectories [16]. A qualitative analysis of the oscillatory motion in the transverse XY plane shows that the wavelength of the channeling trajectory depends on the particle mass M_1 as $\lambda_1 \propto \sqrt{M_1}$. Therefore, we expect a "wavelength ratio" $\sqrt{2}$ for deuterons and $\sim 1/3$ for muons or pions, as compared to protons. This argument explains the behavior observed in Fig. 1.

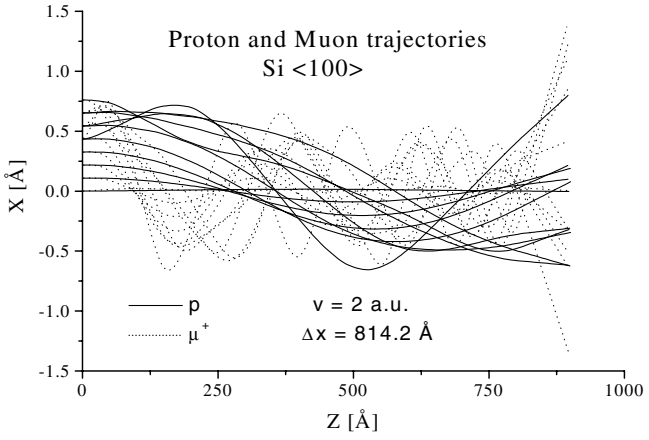

FIG. 1. Trajectories of protons and muons with velocities of 2 a.u., channeled in the $\langle 100 \rangle$ direction of a Si crystal with a thickness of 814.2 Å. The figure shows the projection of trajectories on the ZX plane, where the Z axis coincides with the channel axis. A small set of trajectories with uniform initial spacing relative to the channel axis has been selected only for illustrative purposes.

We also find that with increasing impact parameters (relative to the channel center) the light particles are more probably scattered out and yield larger dechanneling fractions. Therefore, when the trajectories of a large number of transmitted particles are studied, one observes that the flux of light particles is concentrated near the channel axis, whereas heavier particles are spread over wider regions.

Spectra of energy losses are shown in Fig. 2, which shows energy loss distributions for particles with incident velocity $v = 1$ a.u. [Fig. 2(a)], emerging from a crystal of thickness 407.1 Å. We observe an important systematic left shift of the spectra following the order of decreasing mass, so that muons have the lowest energy loss and deuterons the largest. The same behavior is observed in the widths of the distributions (energy straggling). However, similar simulations at higher velocities [$v = 3$ a.u., Fig. 2(b)] show no differences in the spectra.

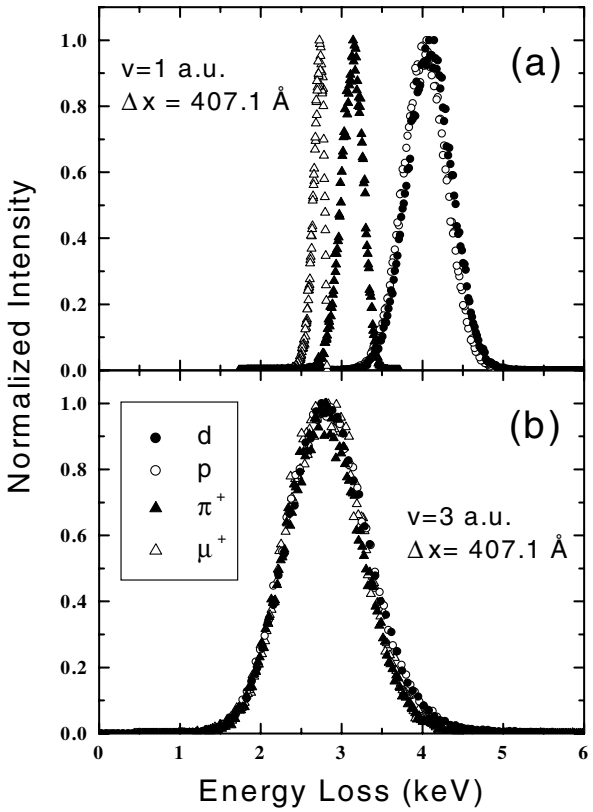

FIG. 2. Energy loss spectra of particles channeled along the $\langle 100 \rangle$ direction of a Si crystal of thicknesses $\Delta x = 407.1$ Å, with equal incident velocities $v = 1$ (a) and $v = 3$ a.u. (b). The simulations correspond to deuterons, protons, pions, and muons, as indicated.

Further simulations were repeated for each particle and for many incident energies. Figure 3(a) shows the results obtained for the mean energy loss of the various particles as a function of the incident energy per unit mass E_1/M_1 (using equal incident velocities for all the particles). The curve corresponding to random stopping, Eq. (4), is also shown for comparison. We observe a large separation of the results for the various particles and a shift in the maximum of the stopping curves for the light ions. We also show the experimental results of proton channeling in Si $\langle 100 \rangle$ at 0.625 and 1.0 MeV from Ref. [17]. In addition, we show in the figure a simple model calculation (solid curve) based on the previous equations but considering a homogeneous electron gas with $r_s = 2.15$ at low energies and $r_s = 1.97$ at high energies. The second r_s value is the one corresponding to the mean valence electron density of Si, whereas the first (fitting) value represents a lower density seen by slow channeled particles. The curve provides in this case only a fair description. The systematic deviations of the simulation results indicate a clear effect of the finite particle mass. Since this effect is most important at low energies, we consider the low-energy scaling of the energy loss in the target [18], $\Delta E = K\bar{v}$, where $\bar{v} = (v_1 + v_2)/2$ is the average between the incident (v_1) and the exit (v_2) velocities for each particle [the friction coefficient $K \equiv K(r_s)$ is assumed equal for all the particles]. In Fig. 3(b) we plot the same results as a function of the equivalent mean energy $\bar{E}/M_1$ defined by $\sqrt{\bar{E}} = (\sqrt{E_1} + \sqrt{E_2})/2$. We observe here a very good alignment of the data points for protons and deuterons and a remarkable agreement with the solid curve (for the chosen r_s values), whereas the results for pions and muons still show systematic deviations. We note that the mean-energy correction introduced before does not affect the high-energy results. To complete this comparison we also show in the figure the experimental data points for proton channeling [17] and for amorphous Si targets [19], which are also in good agreement with the corresponding model calculations.

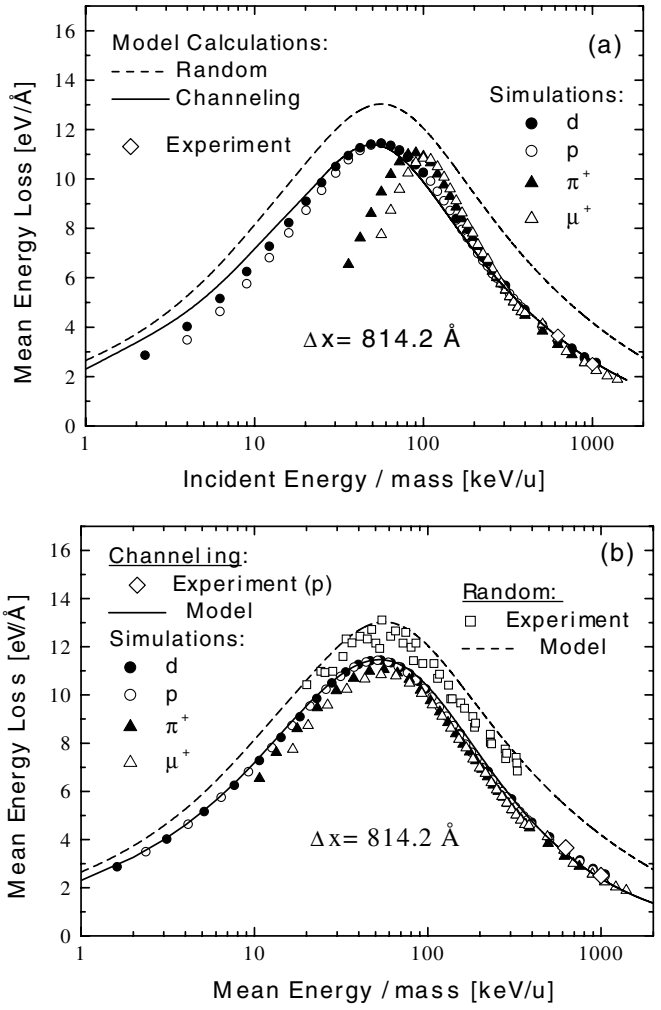

FIG. 3. (a) Mean energy loss of channeled particles in the $\langle 100 \rangle$ direction of Si (with thickness $\Delta x = 814.2$ Å), as a function of the incident energy per unit mass E_1/M_1. Each point is the average energy loss for a large number of simulations obtained from energy spectra similar to those of Fig. 2. The solid and dashed lines are the results of the model described in the text. The diamond symbols at high energies show experimental data for proton channeling. (b) Same results shown as a function of the mean energy $\bar{E}/M_1$, defined in the text. The square data points show experimental results for protons in amorphous Si included for comparison.

A similar study was made for the straggling of the energy loss distributions of emerging particles. In Fig. 4 we show the results of the present simulations together with the simple model described before. In this case, the results have been represented taking into account the low-energy behavior of the energy straggling (which applies both in the linear [11] and nonlinear formulations [13]): $\Omega^2/\delta x = Qv^2$, where the coefficient Q depends only on r_s. By

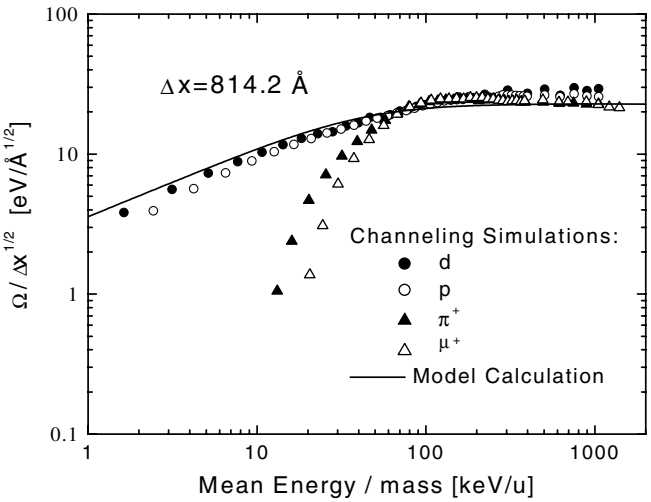

FIG. 4. Straggling values $\Omega/\Delta x^{1/2}$ for particles channeled along the $\langle 100 \rangle$ direction of Si (with thickness $\Delta x = 814.2$ Å) as a function of the mean energy per unit mass $\bar{E}'/M_1$, defined in the text. The solid line shows the simple model calculation described in the text.

integrating the accumulated straggling for a finite foil thickness, $\Omega^2_{\text{foil}}/\Delta x$, it may be shown that this value scales according to a mean energy $\bar{E}' = (E_1 + E_2 + \sqrt{E_1 E_2})/3$. The values shown in Fig. 4 have been represented according to this mean energy criterion. By comparing these results with those of Fig. 3 we observe here more pronounced deviations, indicating a much larger mass effect.

These results predict important mass effects in the energy loss distributions for the light hydrogenlike particles under channeling conditions. The large differences found in this work are produced by two effects: first, the finite energy loss effects arising from the slowing down process in the foil, and second, the effects of dechanneling which are more important for the light particles (muons and pions), as they have higher oscillation frequencies and also a greater chance of being scattered out. As a result of this, the transmitted particles are mostly those with trajectories close to the channel axis; these particles suffer less energy losses and straggling.

We may further illustrate the differences in transmitted fractions of channeled particles with some values obtained from our simulations: for incident muon energies of 20 keV ($\sim$200 keV/u) we find that a fraction of 80%, out of the initial number of channeled particles, survives in channeling trajectories after traversing the 814.2 Å thickness; whereas for an incident energy of 10 keV this fraction reduces to 40%. At lower energies this fraction is further reduced, and we do not observe channeling of muons below 5 keV. On the other hand, in the case of protons the survival fraction of channeled particles remains over 95%, showing no changes over the corresponding energy range.

In summary, contrary to previous results and assumptions for the energy loss in amorphous or polycrystalline media, we find here important mass effects on the energy loss distributions for channeled particles in a wide range of velocities. This is a new effect produced by the channeling process. The recent advances in experimental techniques to produce medium- and low-energy muon beams [3] may provide the possibility of experimentally studying these effects.

We acknowledge financial support by FONDECYT and MIDEPLAN Millenium (Project No. P99-135F), Chile, and ANPCYT (No. PICT03-03579), Argentina.

[1] K. Maier *et al.,* Phys. Lett. **83A**, 341 (1981).
[2] G. Fabritius *et al.,* Nucl. Instrum. Methods Phys. Res., Sect. B **33**, 49 (1988).
[3] E. Morenzoni, Z. Phys. **56**, S243 (1992).
[4] B. D. Patterson, Rev. Mod. Phys. **60**, 69 (1988).
[5] J. Major, A. Seeger, and Th. Stammler, Z. Phys. **56**, S269 (1992).
[6] G. Flik *et al.,* Phys. Rev. Lett. **57**, 563 (1986).
[7] J. F. Ziegler, J. P. Biersack, and U. Littmark, *The Stopping and Ranges of Ions in Solids* (Pergamon, New York, 1985).
[8] D. S. Gemmell, Rev. Mod. Phys. **46**, 129 (1974).
[9] P. Vargas, J. E. Valdés, and N. R. Arista, Phys. Rev. A **53**, 1638 (1996); **56**, 4781 (1997).
[10] O. K. Andersen and O. Jepsen, Phys. Rev. Lett. **53**, 2571 (1984); O. K. Andersen, Z. Pawlowska, and O. Jepsen, Phys. Rev. B **34**, 5253 (1986).
[11] J. Lindhard, Mater. Fys. Medd. K. Dan. Vidensk. Selsk. **28**, No. 8 (1954).
[12] T. L. Ferrell and R. H. Ritchie, Phys. Rev. B **16**, 115 (1977).
[13] J. C. Ashley, A. Gras-Martí, and P. M. Echenique, Phys. Rev. A **34**, 2495 (1986).
[14] J. Calera-Rubio, A. Gras-Martí, and N. R. Arista, Nucl. Instrum. Methods Phys. Res., Sect. B **93**, 137 (1994).
[15] J. Lindhard, Mater. Fys. Medd. K. Dan. Vidensk. Selsk. **34**, No. 14 (1965).
[16] H. F. Krause *et al.,* Phys. Rev. A **49**, 283 (1994).
[17] A. Dygo *et al.,* Nucl. Instrum. Methods Phys. Res., Sect. B **93**, 117 (1994); Z. Y. Zhao *et al.,* Phys. Rev. A **57**, 2742 (1998).
[18] R. Blume, W. Eckstein, and H. Verbeek, Nucl. Instrum. Methods Phys. Res. **194**, 67 (1982).
[19] P. Mertens and P. Bauer, Nucl. Instrum. Methods Phys. Res., Sect. B **33**, 133 (1988).